Available online at www.sciencedirect.com

SciVerse ScienceDirect

Ceramics International 39 (2013) 1189–1194

CERAMICS INTERNATIONAL

www.elsevier.com/locate/ceramint

Rapid synthesis of ZnO nanostructures through microwave heating process

Ian Y.Y. Bu*

Department of Microelectronics Engineering, National Kaohsiung Marine University, 81157 Nanzih District, Kaohsiung City, Taiwan, Republic of China

Received 18 June 2012; received in revised form 13 July 2012; accepted 13 July 2012
Available online 20 July 2012

Abstract

In this paper, polycrystalline zinc oxide (ZnO) nanostructures have been prepared by a hydrothermal synthesis through rapid microwave heating (180 s). The structure, composition and optical properties of the products were examined by scanning electron microscopy (SEM), energy dispersive x-ray spectrum (EDS), ultraviolet–visible spectroscopy (UV–vis), x-ray diffraction (XRD), photoluminescence spectroscopy (PL) and Raman spectroscopy. Typically, the synthesized nanostructures were zinc-rich with diameter ranging from 20 nm to 200 nm in length. From the Raman spectroscopy and PL measurements, it was found that the as-deposited films contain vacancy defects that originated from the rapid synthesis process.

Keywords: A. Microwave processing; B. Nanocomposites; C. Optical properties; D. ZnO

1. Introduction

Zinc oxide (ZnO) is a wide bandgap (3.37 eV) semiconductor with large exciton binding energy that has been used in wide range of applications such as photovoltaic [1,2], sensors [3–5], thin film transistors [6,7], humidity sensing [8] and nano-generators [9]. One of the attractive features of ZnO is the wide range of nanostructure it can adapt through control of process parameters. Previous studies have successfully synthesized nanowires [10–13], nanorods [14–17], nanopetals [18,19], and nanotripods [20].

Several methods have been adapted to prepare ZnO nanostructures such as thermal chemical vapor deposition (CVD) over catalyst coated substrates [21,22], electrochemical process on anodized alumina membrane [23] and hydrothermal growth on pre-seeded layer [24,25]. Although high quality ZnO nanomaterials can be obtained through thermal CVD process, excessive process temperature and complicated vacuum equipment presents major up-scaling and cost related issues. Alternatively, an anodized alumina membrane process presents versatile template process for manufacturing ZnO and can be adapted to wide range of nanomaterials (cadmium telluride [26], ZnO [27], copper indium gallium selenide [28] etc.). However, high-quality anodized alumina membrane is expensive and suffers from scaling issues. On the other hand, hydrothermal process is an attractive process due to its low technological requirements and low-process temperature ($< 100\ ^{\circ}C$) that enables depositions on low-cost, flexible plastic substrates. Generally, hydrothermal process consists of two steps; namely, seed layer deposition and ZnO growth. Firstly, the seed layer is prepared by refluxing ZnO containing compounds (e.g. zinc acetate) in alcoholic solvent. Subsequently, the prepared solution is spin coated onto the substrate and annealed to enable conformal seed layer formation. The second step, consists of transferring the pre-coated substrate into heated chemical bath which consists of zinc nitrate and ammonia-based nutrient solution (hexamine). After the nutrient solution is replenished, the growth rate of ZnO nanostructures slows down and eventually terminates. In order to produce ZnO nanowires with practical length (5 μm) typical growth time lasts for 2–12 h [25]. Such slow deposition rate is impractical for industrial production.

Consequently, it would be attractive to find the growth of ZnO nanomaterials accelerate through alternative deposition techniques. Microwave assisted process has been of interest ever since the first reports [29,30]. Noteworthy features include rapid volumetric heating and

*Tel.: +886 97250 6900; fax: +886 73645589.
E-mail address: ianbu@hotmail.com

0272-8842/$ - see front matter © 2012 Elsevier Ltd and Techna Group S.r.l. All rights reserved.
http://dx.doi.org/10.1016/j.ceramint.2012.07.043

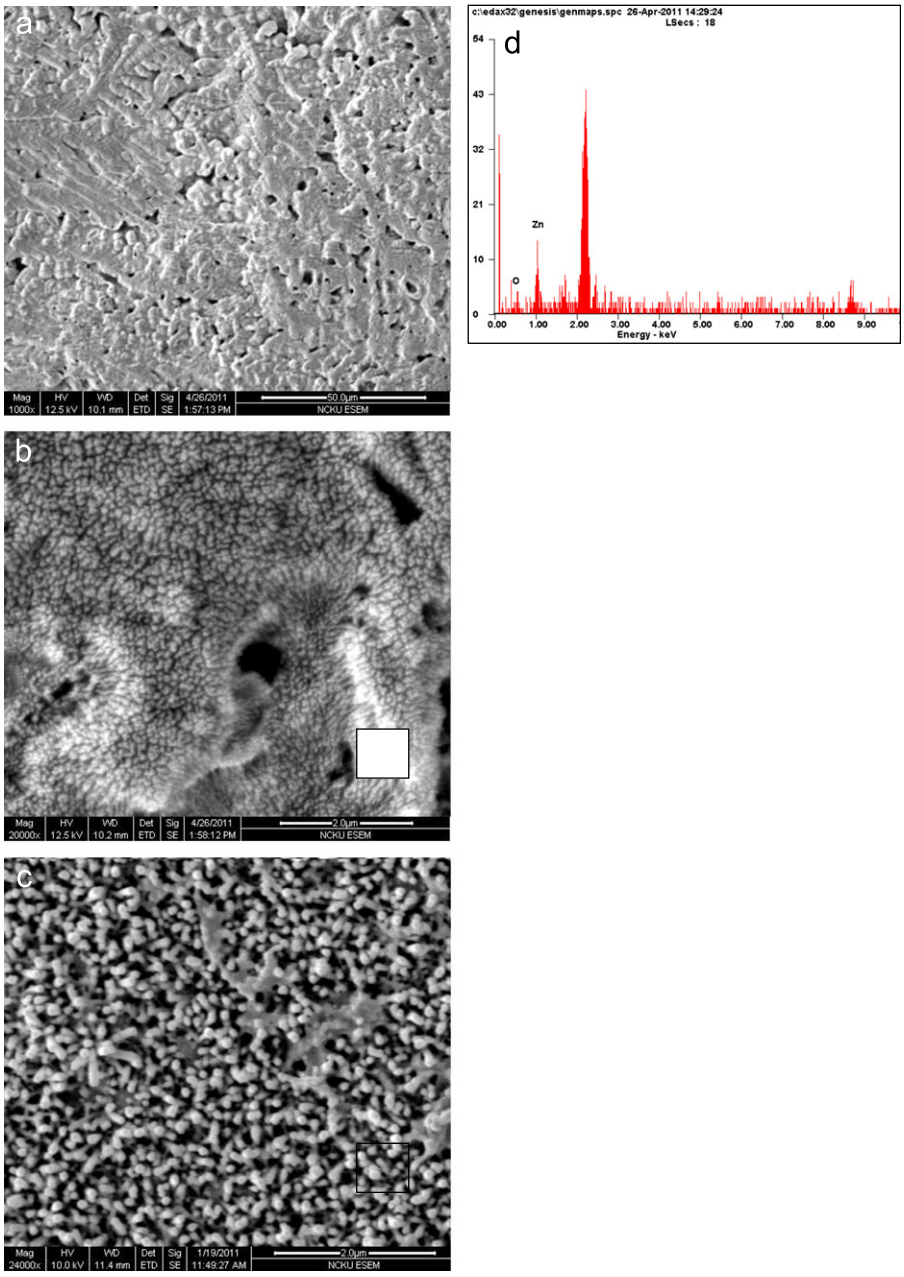

Fig. 1. (a) Top view SEM image of the as deposited ZnO nanostructure at lower resolution. (b) Top view SEM image of the as-deposited ZnO nanostructure at higher resolution. (c) Typical top view SEM image of the hydrothermally grown ZnO nanowire by hot-plate heating. (d) Typical EDS composition analysis of the microwave synthesized ZnO.

energy saving as compared to conventional heating methods. Consequently, microwave assisted heating has been adapted to synthesis various nanocrystalline ZnO oxide. In this study, a one pot, fast synthesis method of zinc oxide nanomaterials by microwave irradiation has been developed and thoroughly characterized through SEM, EDS, UV–vis, XRD, PL and Raman spectroscopy.

2. Experimental

All chemicals were of analytical grade, purchased from Sigma Aldrich and used without further purification. In a typical procedure, soda lime glasses were sequentially cleaned by ultrasonication in acetone, methanol and deionized water (DI). The cleaned soda lime glass substrates were blown dry by N_2 flow and coated with ZnO seed layer by spinner. The ZnO seed layer solution was prepared by dissolving 1 mM of zinc acetate into IPA using a magnetic stirrer without external heating. Then, the spin-coated seed layer is heated to 300 °C for 10 min to ensure the formation of nano-sized ZnO seed. Such coating and annealing of seed layer were repeated three cycles to enhance adhesion to the substrates.

The seed-coated glass substrates were transferred into the growth solution (equimolar aqueous solution of zinc

nitrate and hexamine). Hydrothermal growths for ZnO NWs (HGZN) were performed at 90 °C bath temperature for 2 h. On the other hand, microwave synthesized zinc nanowires were performed at 140 W for 180 s, using a commercially available microwave oven (Eupa). It must be emphasized that both samples were prepared with exact condition until the hydrothermal growth. Obviously, the major differences between the samples were the source of thermal excitation.

In the case for microwave synthesis, the microwave irradiation results in white solid (ZnO) precipitations with complete evaporation of solvents. These collected precipitates were repeatedly washed by ultrasonic bath in D.I. water and dispersed in IPA to yield microwave-processed solution (MPS). Subsequently, MPS was spin coated onto glass substrate and heated to 120 °C to remove solvents.

The chemical composition and structure of the ZnO nanowire samples were determined by using an FEI Quanta 400F Environmental Scanning Electron Microscope (ESEM), equipped with an Energy Dispersive Spectroscopy (EDS). Crystal orientation was measured by the Siemens D5000 X-Ray Diffractometer which uses the Cu Kα radiation. Raman spectroscopy and photoluminescence of the samples were evaluated by the Dongwoo Macro Raman spectrometer/PL system at room temperature.

3. Discussion

Fig. 1(a) shows the SEM image of the microwave synthesized ZnO thin films at lower magnification. It can be observed that the typical morphology of the film is ZnO agglomerations with voids. Fig. 1(b) shows the SEM image of the same film at a higher resolution. Upon closer examination, one-dimensional nanowires can be observed clearly from Fig. 1(b) with length and diameter of the ZnO estimated to be around 200 nm and 20 nm, respectively. Fig. 1(c) shows the EDS compositional analysis on the microwave synthesized ZnO. Generally, the deposited film is Zn rich with Zn/O ratio if 57.7/42.3. This data correlate well with previous microwave studies on ZnO synthesis and have revealed that hydrothermally grown ZnO tends to be slightly Zn rich. Fig. 1(d) shows the top-view representative SEM image of hydrothermally grown ZnO nanowires through hotplate heating process. It can be observed from Fig. 1(d) that the samples prepared through hotplate heating is ordered and showed vertical alignment to the substrate.

Fig. 2 presents the XRD pattern of the microwave synthesized films. The pronounced ZnO peaks at (100), (002), (101), (102) and (200) appeared at 2θ 31.9°, 34.4°, 37.3°, 48.1° and 66.7°, respectively. Several peaks attributed to zinc acetate (JCPDS No. 01-0089) were also present in the XRD pattern and marked with x. The XRD pattern suggests the as deposited films consists of mixture of crystalline ZnO with zinc acetate.

Typically, hydrothermally grown ZnO thin films are crystallized without significant zinc acetate residuals. This is due to

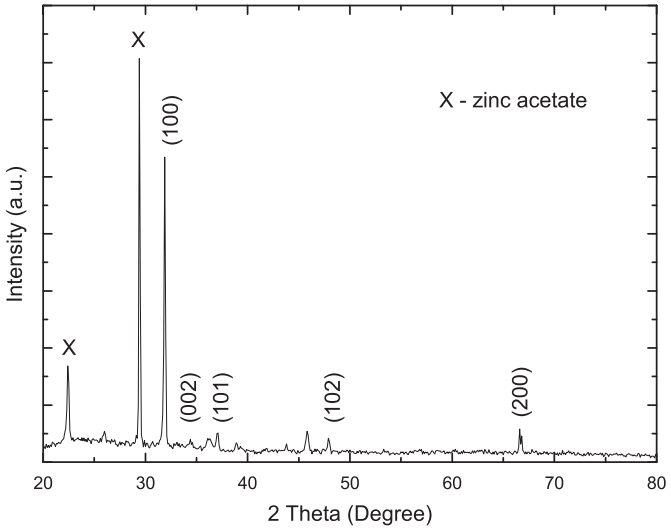

Fig. 2. Typical XRD pattern of microwave synthesized ZnO nanostructure thin film.

annealing of seed layer at temperature in excess of 300 °C, which eliminates the organic compounds and transforms the zinc acetate into ZnO. Whereas in our process, the synthesizing low temperature (90 °C) and short reaction time (180 s) results in incomplete transformation of zinc acetate. Zinc acetate dehydrate sublimes at around 175 °C, melts at 250 °C and fully converts into ZnO by 300 °C. Fig. 3(a) shows the transmittance for spectra of ZnO films on glass substrate with microwave and conventionally hydrothermally grown ZnO nanowires. The microwave synthesized ZnO nanostructures exhibit transmittance of around 60% between wavelength of 400–800 nm with marginal increase in transmittance to 65% at 1200 nm. Whereas conventionally hydrothermally grown ZnO nanowires exhibited gradual increase in optical transmittance (30–60%) from wavelength range of 400–600 nm. Such trend continued and reached maximum transmittance of around 70% at 1200 nm. In the solar cell industry, ZnO prepared by sputtering are atomically smooth and highly transparent in the visible region. In order to reduce light loss and enhance the power conversion efficiency, antireflective layers are built onto the front surface of solar cells via wet or dry surface texturing. In most of the investigations antireflection layers have been attributed to enhanced probability of absorption by the nanostructures. In the case of hydrothermally grown ZnO, the well ordered nanostructure effectively traps the light and reduces transmittance. In contrast, microwave synthesized ZnO nanostructures traps light at much lower rate due to the reduction in length, which reduces light scattering. Optical band gap (Tauc gap) can be obtained by analyzing the absorption edge and apply the Tauc model

$$(\alpha h\nu) = A\left(h\nu - E_g\right)^{1/2}$$

where α is the absorption coefficient, $h\nu$ is the photon energy, and A is a constant and E_g is the bandgap. The optical bandgap of ZnO films prepared by the hydrothermal

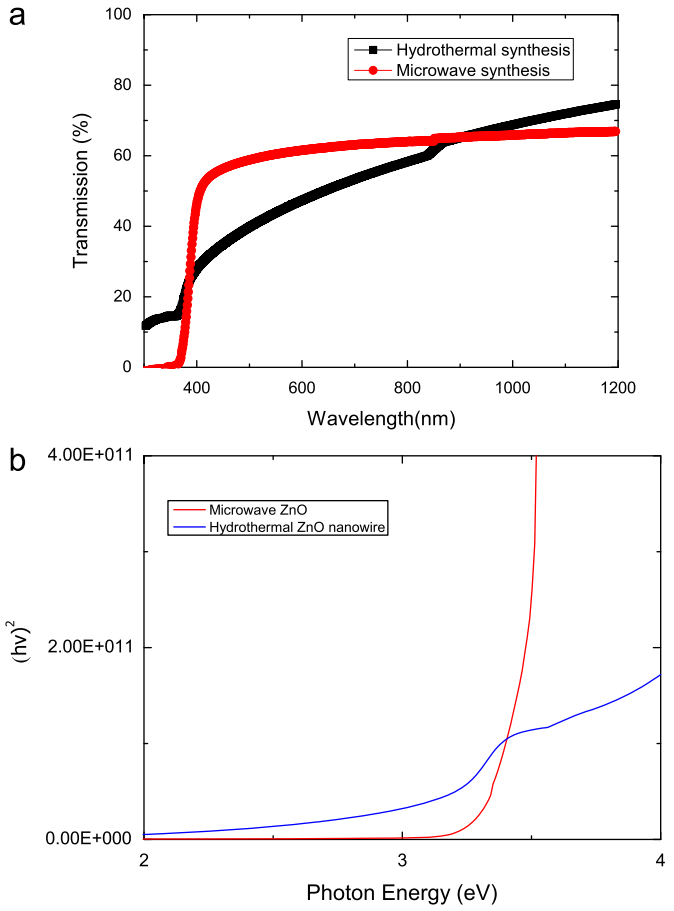

Fig. 3. (a) Comparison of transmittance of hot-plate and microwave heated ZnO and (b) Corresponding extraction of the bandgap through steps described in text.

method and microwave heating was determined by extrapolating the slope from the plot in Fig. 3(a). From Fig. 3(b), the extracted bandgap from the Tauc plot for microwave synthesized ZnO was 3.29 eV very close to the bandgap of ZnO crystal (3.3 eV). Whereas extracted bandgap for hydrothermally grown ZnO naowires were determined to be around 3.03 eV. Although previous studies attribute the shift in bandgap to structural defects and grain boundaries, we believe additional mechanism may come into play. The enhanced light scattering through the ZnO nanowire may have contributed significantly to the shift.

PL spectroscopy is a useful tool to determine the structural properties of ZnO film. Generally, two peaks can be used to determine the quality of deposited ZnO film. The green emission peaks, centered at around 550 nm, are related to oxygen vacancy defects. Whereas, the peak positioned around 385 nm is termed near band emission and an indication of high quality ZnO. In the case of hydrothermally grown ZnO nanowires, a sharp peak at 385 nm accompanied by a broad peak can be observed in Fig. 4. The quality of ZnO can be evaluated by the ratio of integrated peaks at I_{385} and I_{550}. I_{385}/I_{500} is determined to be around 1.38, which indicate good crystalline structure. On the other hand, microwave

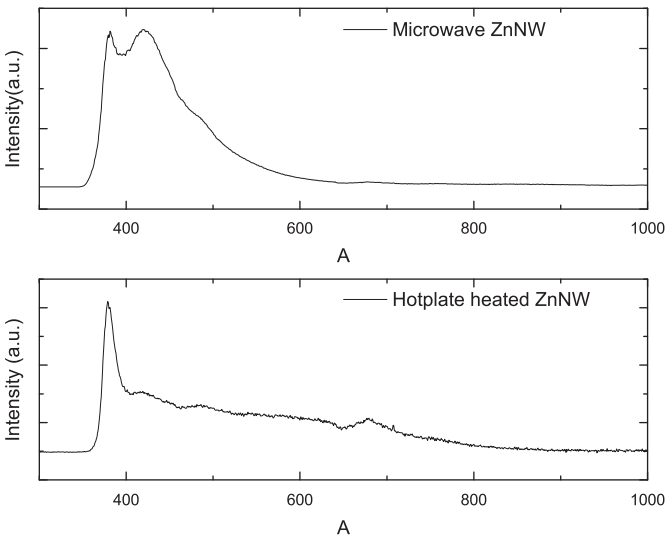

Fig. 4. PL spectra of the microwave and hot-plate synthesized ZnO.

synthesized ZnO exhibit peaks at around 385, 425, and 500 nm. Which means, apart from the high quality ZnO formation, other phases (such as vacancies and interstitial-related defects) may have also formed. This data correlate well with XRD peak and indicates that several different phases have formed. The unidentified peak at 425 nm are believed to have originated from zinc interstitial defects and can be removed by post-deposition thermal annealing.

Raman spectroscopy is a powerful tool that can illuminate the microstructure features of the deposited films. Fig. 5 shows the Raman spectrum of the hot plate synthesized and microwave synthesized ZnO samples. From the Raman spectrum, four major peaks can be observed, centered at 477. 577, 819 and 1732 cm^{-1}. The peak centered at around 477 cm^{-1} can be attributed to the glass substrate. The 577, 819 and 1732 cm^{-1} peaks can be attributed to Raman LO phonon scattering and its overtones. It is also interesting to note that a small peak centered at around 65 cm^{-1} is present in hotplate synthesized samples, which are absent in microwave synthesized ZnO samples. However, the peak centered at 65 cm^{-1} are termed as the Bosons peak [31] and originated from breakdown of crystal symmetries, which prevents distinctions between optical and acoustic modes in the lower frequency. Although the main differences in the samples are the deposition procedures, it is believed that the observed Bosons peaks are related to phonon propagation in the glass. The absence of such peak in microwave heated samples is probably due to better coverage of the deposited material.

In general, the bandgap of the ZnO thin films is around 3.24 eV, much lower than the excitation photon energy 3.8 eV. Under such experimental condition, LO and LO overtones dominants over Raman spectras which resulted from the enhancement of the Fróhlich interaction, due to the similarity of scattered-photon energy by *n*-LO phonon with that of exciton energy. The peaks observed in our films are in good agreement with that of the single crystal *c*-axis oriented ZnO. This further supports the *c*-axis

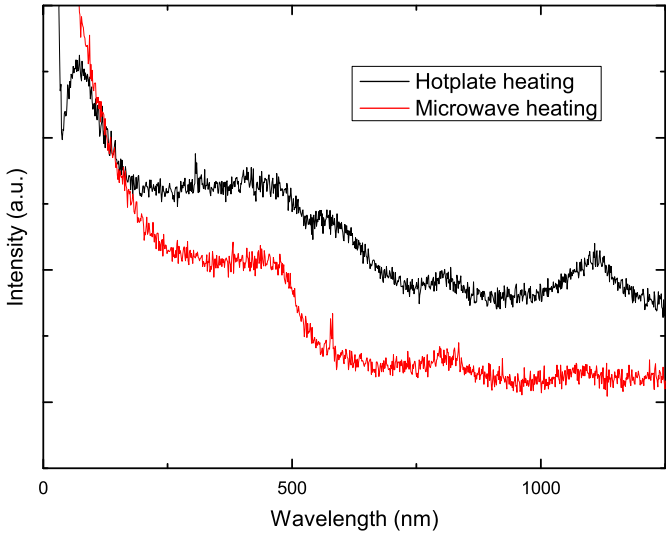

Fig. 5. Comparison of the Raman spectra of the microwave and hot-plate heated ZnO.

preferential orientation of the synthesied ZnO nanowires and correlate with XRD and SEM data. The Raman shift peak at 577 cm^{-1} is only prominent in microwave synthesized ZnO thin film and originate from oxygen vacancies or Zn interstitials. Such peak is absent within hydrothermally grown ZnO nanowires due to structuring during thermal annealing process.

4. Conclusion

High quality and transparent thin films of intrinsic ZnO nanostructures have been deposited onto the glass by a microwave process. The sintered ZnO films consists of nanowires with aspect ratio of 10. Compositionwise the derived ZnO nanowire is Zn rich. Conventionally, hydrothermally grown ZnO films exhibit preferential growth in the 002 orientation due to the suppression of growth in other phases via addition of hexamine. In contrast, microwave synthesized ZnO consists of mixed phases XRD peaks at (100), (002), (101), (102) and (200). The XRD patterns also suggest residual zinc acetate from the incomplete reaction. This is probably from the short and not optimized condition and can be reduced or eliminated by changing parameters such as deposition power, duration etc. Room temperature PL measurements also confirm the formation of mixed phase material with NBE at 380 cm^{-1} and additional peaks at 425 and 500 nm. Raman spectroscopy indicates that not optimized microwave synthezised ZnO nanowire is the *c*-axis oriented and contains oxygen interstitial or zinc vacancies.

Acknowledgment

The author I.Y.Y. Bu would like to thank National Science Council for financial support under the Grant number NSC 99-2628-E-022-001.

References

[1] K.A. Salman, K. Omar, Z. Hassan, Improved performance of a crystalline silicon solar cell based on ZnO/PS anti-reflection coating layers, Superlattices and Microstructures 50 (5) (2011) 517–528.
[2] S.E. Pust, J.P. Becker, J. Worbs, S.O. Klemm, K.J.J. Mayrhofer, J. Hüpkes, Electrochemical etching of zinc oxide for silicon thin film solar cell applications, Journal of the Electrochemical Society 158 (2011) 41–55.
[3] B. de Lacy Costello, R. Ewen, N.M. Ratcliffe, M. Richards, Highly sensitive room temperature sensors based on the UV-LED activation of zinc oxide nanoparticles, Sensors and Actuators B: Chemical 134 (2008) 945–952.
[4] O. Lupan, L. Chow, S. Shishiyanu, E. Monaico, T. Shishiyanu, V. Sontea, B. Roldan Cuenya, A. Naitabdi, S. Park, A. Schulte, Nanostructured zinc oxide films synthesized by successive chemical solution deposition for gas sensor applications, Materials Research Bulletin 44 (2009) 63–69.
[5] N. Hongsith, C. Viriyaworasakul, P. Mangkorntong, N. Mangkorntong, S. Choopun, Ethanol sensor based on ZnO and Au-doped ZnO nanowires, Ceramics International 34 (2008) 823–826.
[6] J. Li, F. Zhou, H.P. Lin, W.Q. Zhu, J.H. Zhang, X.Y. Jiang, Z.L. Zhang, Enhanced photosensitivity of InGaZnO-TFT with a CuPc light absorption layer, Superlattices and Microstructures 51 (4) (2012) 538–543.
[7] H.H. Hsieh, T.T. Tsai, C.Y. Chang, S.F. Hsu, C.S. Chuang, Y. Lin, Activematrix organic lightemitting diode displays with indium gallium zinc oxide thinfilm transistors and normal, inverted, and transparent organic lightemitting diodes, Journal of the Society for Information Display 19 (2011) 323–328.
[8] I.Y.Y. Bu, C.C. Yang, High-performance ZnO nanoflake moisture sensor, Superlattices and Microstructures 51 (6) (2012) 745–753.
[9] M.P. Lu, J. Song, M.Y. Lu, M.T. Chen, Y. Gao, L.J. Chen, Z.L. Wang, Piezoelectric nanogenerator using p-type ZnO nanowire arrays, Nano Letters 9 (2009) 1223–1227.
[10] I.Y.Y. Bu, Y.M. Yeh, Effects of sulfidation on the optoelectronic properties of hydrothermally synthesized ZnO nanowires, Ceramics International 38 (5) (2012) 3869–3873.
[11] M.H. Huang, Y. Wu, H. Feick, N. Tran, E. Weber, P. Yang, Catalytic growth of zinc oxide nanowires by vapor transport, Advanced Materials 13 (2001) 113–116.
[12] C. Lee, T. Lee, S. Lyu, Y. Zhang, H. Ruh, H. Lee, Field emission from well-aligned zinc oxide nanowires grown at low temperature, Applied Physics Letters 81 (2002) 3648–3650.
[13] H. Lu, X. Yu, Z. Zeng, D. Chen, K. Bao, L. Zhang, H. Wang, H. Xu, R. Zhang, DC-field-induced synthesis of ZnO nanowhiskers in water-in-oil microemulsions, Ceramics International 37 (2011) 287–292.
[14] M. Willander, O. Nur, Q. Zhao, L. Yang, M. Lorenz, B. Cao, P.J. Zuniga, C. Czekalla, G. Zimmermann, M. Grundmann, Zinc oxide nanorod based photonic devices: recent progress in growth, light emitting diodes and lasers, Nanotechnology 20 (2009) 332001.
[15] Y. Zhang, K. Yu, D. Jiang, Z. Zhu, H. Geng, L. Luo, Zinc oxide nanorod and nanowire for humidity sensor, Applied Surface Science 242 (2005) 212–217.
[16] T.K. Roy, D. Bhowmick, D. Sanyal, A. Chakrabarti, Sintering studies of nano-crystalline zinc oxide, Ceramics International 34 (2008) 81–87.
[17] P. Amornpitoksuk, S. Suwanboon, S. Sangkanu, A. Sukhoom, N. Muensit, Morphology, photocatalytic and antibacterial activities of radial spherical ZnO nanorods controlled with a diblock copolymer, Superlattices and Microstructures 51 (1) (2011) 103–113.
[18] Q. Ahsanulhaq, S. Kim, J. Kim, Y. Hahn, Structural properties and growth mechanism of flower-like ZnO structures obtained by simple solution method, Materials Research Bulletin 43 (2008) 3483–3489.
[19] H.R. Pant, C.H. Park, B. Pant, L.D. Tijing, H.Y. Kim, C.S. Kim, Synthesis, characterization, and photocatalytic properties of ZnO nano-flower containing TiO_2 NPs, Ceramics International (2011).

[20] A. Wisitsoraat, I. Pimtara, D. Phokharatkul, K. Jaruwongrangsee, A. Tuantranont, Zinc oxide nanopolypods synthesized by thermal evaporation of carbon nanotubes and zinc oxide mixed powder, Current Nanoscience 6 (2010) 45–53.
[21] B. Xiang, P. Wang, X. Zhang, Shadi.A. Dayeh, D.P.R. Aplin, C. Soci, D. Yu, D. Wang, Rational synthesis of p-type zinc oxide nanowire arrays using simple chemical vapor deposition, Nano Letters 7 (2007) 323–328.
[22] J.H. Zeng, Y.L. Yu, Y.F. Wang, T.J. Lou, High-density arrays of low-defect-concentration zinc oxide nanowire grown on transparent conducting oxide glass substrate by chemical vapor deposition, Acta Materialia 57 (2009) 1813–1820.
[23] L. Li, N. Koshizaki, G. Li, Nanotube arrays in porous anodic alumina membranes, Journal of Materials Science and Technology 24 (2008) 551–562.
[24] J. Joo, B.Y. Chow, M. Prakash, E.S. Boyden, J.M. Jacobson, Face-selective electrostatic control of hydrothermal zinc oxide nanowire synthesis, Nature Materials 10 (2011) 596–601.
[25] H.E. Unalan, P. Hiralal, N. Rupesinghe, S. Dalal, W.I. Milne, G.A.J. Amaratunga, Rapid synthesis of aligned zinc oxide nanowires, Nanotechnology 19 (2008) 255608.
[26] Z. Fan, H. Razavi, J. Do, A. Moriwaki, O. Ergen, Y.L. Chueh, P.W. Leu, J.C. Ho, T. Takahashi, L.A. Reichertz, Three-dimensional nanopillar-array photovoltaics on low-cost and flexible substrates, Nature Materials 8 (2009) 648–653.
[27] B. Gao, H.M. Zhang, X.J. Li, G.F. Hu, Y.J. Li, Y.J. Zhu, Fabrication of ZnO nanodot arrays by sol–gel within AAO template, Advanced Materials Research 150 (2011) 921–925.
[28] R. Inguanta, P. Livreri, S. Piazza, C. Sunseri, Fabrication and photoelectrochemical behavior of ordered CIGS nanowire arrays for application in solar cells, Electrochemical Solid State Letters 13 (2010) 22–25.
[29] R.J. Giguere, T.L. Bray, S.M. Duncan George, Application of commercial microwave ovens to organic synthesis. 1, Tetrahedron Letters 27 (1986) 4945–4948.
[30] R. Gedye, F. Smith, K. Westaway, H. Ali, L. Baldisera, L. Laberge, J. Rousell, The use of microwave ovens for rapid organic synthesis, Tetrahedron Letters 27 (1986) 279–282.
[31] E. Duval, A. Boukenter, T. Achibat, Vibrational dynamics and the structure of glasses, Journal of Physics: Condensed Matter 2 (1990) 10227.